Neurobiology of Aging 72 (2018) 72–82

Contents lists available at ScienceDirect

Neurobiology of Aging

journal homepage: www.elsevier.com/locate/neuaging

In vivo mapping of brainstem nuclei functional connectivity disruption in Alzheimer's disease

Laura Serra [a,1], Marcello D'Amelio [b,c,1], Carlotta Di Domenico [a], Ottavia Dipasquale [d], Camillo Marra [e], Nicola Biagio Mercuri [f,g], Carlo Caltagirone [g,h], Mara Cercignani [a,i], Marco Bozzali [a,i,*]

[a] Neuroimaging Laboratory, IRCCS Santa Lucia Foundation, Rome, Italy
[b] Laboratory Molecular Neurosciences, IRCCS Santa Lucia Foundation, Rome, Italy
[c] Unit of Molecular Neurosciences, Department of Medicine, University Campus-Biomedico, Rome, Italy
[d] Department of Neuroimaging, Institute of Psychiatry, Psychology and Neuroscience, King's College London, London, United Kingdom
[e] Institute of Neurology, Catholic University, Rome, Italy
[f] Laboratory of Experimental Neurology, IRCCS Santa Lucia Foundation, Rome, Italy
[g] Department of Systems Medicine, University of Rome 'Tor Vergata', Rome, Italy
[h] Department of Clinical and Behavioural Neurology, IRCCS Santa Lucia Foundation, Rome, Italy
[i] Department of Neuroscience, Brighton & Sussex Medical School, University of Sussex, Brighton, East Sussex, United Kingdom

ARTICLE INFO

Article history:
Received 19 December 2017
Received in revised form 7 August 2018
Accepted 14 August 2018
Available online 23 August 2018

Keywords:
Alzheimer's disease
VTA
LC
Brain disconnection
Neuropsychiatric symptoms

ABSTRACT

We assessed here functional connectivity changes in the locus coeruleus (LC) and ventral tegmental area (VTA) of patients with Alzheimer's disease (AD). We recruited 169 patients with either AD or amnestic mild cognitive impairment due to AD and 37 elderly controls who underwent cognitive and neuropsychiatric assessments and resting-state functional magnetic resonance imaging at 3T. Connectivity was assessed between LC and VTA and the rest of the brain. In amnestic mild cognitive impairment patients, VTA disconnection was predominant with parietal regions, while in AD patients, it involved the posterior nodes of the default-mode network. We also looked at the association between neuropsychiatric symptoms (assessed by the neuropsychiatric inventory) and VTA connectivity. Symptoms such as agitation, irritability, and disinhibition were associated with VTA connectivity with the parahippocampal gyrus and cerebellar vermis, while sleep and eating disorders were associated with VTA connectivity to the striatum and the insular cortex. This suggests a contribution of VTA degeneration to AD pathophysiology and to the occurrence of neuropsychiatric symptoms. We did not find evidence of LC disconnection, but this could be explained by the size of this nucleus, which makes it difficult to isolate. These results are consistent with animal findings and have potential implications for AD prognosis and therapies.

1. Introduction

Alzheimer's disease (AD) is clinically characterized by neuropsychiatric symptoms in addition to a progressive cognitive decline (Alves et al., 2017). The relevance of neuropsychiatric symptoms has become increasingly evident as demonstrated by their early occurrence in cognitively intact individuals who subsequently develop dementia (Masters et al., 2015). The cholinergic hypothesis (Bartus et al., 1982) of AD has been extensively investigated, showing that cholinergic dysfunctions in the basal forebrain account for memory deficits in typical AD (Theofilas et al., 2015). It has been proposed that AD symptoms may also result from structural and functional abnormalities of the dopaminergic (Theofilas et al., 2015) and noradrenergic (Borodovitsyna et al., 2017) systems. The noradrenergic (Borodovitsyna et al., 2017) or dopaminergic stimulation (Theofilas et al., 2015) leads to a significant improvement of cognitive functions, while their simultaneous stimulation reduces both beta amyloid (Aβ) load and tau pathology (Theofilas et al., 2015). Among the dopaminergic-rich nuclei, the ventral tegmental area (VTA) is known to be part of the reward system (Krebs et al., 2011; Nobili et al., 2017), and dopaminergic VTA

* Corresponding author at: Department of Neuroscience, Brighton and Sussex Medical School, University of Sussex, Brighton, East Sussex, UK. Tel.: 44 (0) 1273 873509; fax: +44 (0) 1273 876721.
E-mail address: m.bozzali@bsms.ac.uk (M. Bozzali).
[1] These authors contributed equally to the article.

https://doi.org/10.1016/j.neurobiolaging.2018.08.012

neurons are critically implicated in the regulation of several functions, ranging from memory and motivational processes (Krebs et al., 2011; Nobili et al., 2017) to sleep-wake behaviors (Eban-Rothschild et al., 2016). Consistently, dopaminergic dysfunctions have been implicated in the occurrence of various neuropsychiatric symptoms, including mood disorders (Ashok et al., 2017; Schaeffer & Berg, 2017), apathy (Chong and Husain, 2016), sleep (Kim et al., 2017), and eating disorders (Kessler et al., 2016). Most noradrenergic neurons originate from the locus coeruleus (LC), whose projections reach the entire cerebral cortex, the thalamic nuclei, and the hippocampus (Robertson et al., 2013). LC undergoes significant functional and structural modifications in AD (Theofilas et al., 2015) as confirmed by postmortem observations (Francis et al., 1985; Storga et al., 1996) and supported by neurophysiological studies (Benussi et al., 2017; Gonsalvez et al., 2017). In postmortem studies, LC has been shown containing hyperphosphorylated tau, the major component of neurofibrillary tangles (NFT), not only in AD patients but also in nondemented individuals decades before the typical age of clinical onset of AD (Braak and Del Tredici, 2011a; Braak and Del Tredici, 2011b; Pamphlett and Kum Jew, 2015). According to this model, hyperphosphorylated tau that forms early on in life in LC neurons would spread via cell-to cell transfer to other neurons to produce NFT (Braak and Del Tredici, 2011a). Damage to the LC with consequent decrease in noradrenaline would also promote the formation of Aβ plaques (Heneka et al., 2006; Pamphlett and Kum Jew, 2015).

Taken together, these data suggest that a loss of monoaminergic neurons might contribute to AD pathophysiology and might explain some of its clinical manifestation, particularly the neuropsychiatric symptoms (Köhler et al., 2016).

A recent study (Nobili et al., 2017), performed in a transgenic mouse model of AD, showed that the progressive degeneration of dopaminergic neurons from VTA results in lower dopamine outflow in the hippocampus and nucleus accumbens, which correlates with deficits in memory and reward processing. Importantly, this dopaminergic loss precedes Aβ plaque deposition, thus representing one of the earliest pathological changes in AD. More recently, evidence of VTA degeneration in association with memory deficits has been provided in patients with AD and mild cognitive impairment (De Marco and Venneri., 2018). Interestingly, a recent resting-state functional magnetic resonance imaging (fMRI) study demonstrated in healthy individuals that VTA and the substantia nigra pars compacta are functionally connected to the default mode network (DMN) (Bär et al., 2016), which is known being selectively disrupted in AD since early clinical stages (Gili et al., 2011). Neuropsychiatric symptoms are also part of the clinical picture of AD since the early disease stages (Serra et al., 2010), and dopaminergic dysfunction is likely to play a pathophysiological relevant role for their manifestation.

We hypothesize that, if a loss of dopaminergic neurons occurs in patients with AD from an early stage, possibly preclinical, and a similar pattern of degeneration occurs to noradrenergic neurons originating from the LC, this neuronal loss should result in lower functional connectivity (FC) between the VTA and/or the LC and the rest of the brain. In addition, these changes likely account for the occurrence and severity of cognitive and behavioral symptoms.

While we are unable to address directly the first 2 hypotheses, we focused on the remaining 2. To interrogate these hypotheses, we recruited a large sample of patients with either AD or amnestic mild cognitive impairment (a-MCI) due to AD, and we used resting-state fMRI as a surrogate measure of neuronal degeneration. fMRI assesses the connectivity between brain areas by measuring the correlation between spontaneous fluctuations in neuronal activity occurring at remote locations (Biswal et al., 1995; Fox et al., 2005). A loss of neurons within a specific nucleus, such as LC or VTA, is expected to result in altered connectivity with its projection areas. It was previously shown that resting-state fMRI may be used to measure the connectivity of small subcortical structures such as the brainstem nuclei (Bianciardi et al., 2018), comparable in size to VTA and LC.

2. Methods

2.1. Participants

A cohort of 169 participants, 84 of them with a diagnosis of probable AD (McKhann et al., 2011) or Alzheimer's clinical syndrome (Jack et al., 2018), 48 with a diagnosis of a-MCI (Albert et al., 2011), and 37 healthy elderly subjects (HS) were enrolled for this study. The diagnosis of probable AD was done according to the clinical criteria of the National Institute of Neurological and Communicative Disorders and Stroke-Alzheimer's Disease and Related Disorders Association (McKhann et al., 2011) and fit with the criteria for Alzheimer's clinical syndrome reported more recently by Jack et al. (2018). The diagnosis of a-MCI was performed according to current available criteria (Albert et al., 2011). Patients with a-MCI could be either single (n = 24) or multiple (n = 24) domains and had not to respond to the diagnostic criteria for major cognitive disorder (American Psychiatric Association (APA), 2013), showing a clinical dementia rating (Hughes et al., 1982) score not exceeding 0.5. Cognitive profile characterized by episodic memory impairment at onset, episodic memory deficit documented at formal testing, and medial temporal lobe atrophy (see Section 2.3.1) confirmed that all individuals had a profile supporting Alzheimer's clinical syndrome at different stages.

Cognitively normal subjects showing the presence of significant medial temporal lobe atrophy were excluded. All recruited subjects with a Hachinski score (Hachinski et al., 1975) higher than 4 were excluded. Major systemic, psychiatric, and other neurological illnesses (with a special attention to Parkinson disease and parkinsonism) were also carefully investigated and excluded in all participants. Finally, subjects had to be right-handed, as assessed by the Edinburgh Handedness Inventory (Büsch et al., 2010). The main demographic and clinical characteristics of the participants are summarized in Table 1, together with data about their medication.

This study was approved by the Ethical Committee of Santa Lucia Foundation, and written informed consent was obtained from all participants before study initiation. All procedures performed in this study were in accordance with the 1964 Helsinki declaration and its later amendments or comparable ethical standards.

2.2. Neuropsychological and behavioral assessment

All participants underwent an extensive neuropsychological battery covering all cognitive domains, which included (1) verbal episodic long-term memory: 15-Word List (immediate, 15-minute delayed recall and recognition) (Carlesimo et al., 1996); Short Story Test (immediate and 20-minute delayed recall) (Carlesimo et al., 2002); (2) visuospatial long-term memory: Complex Rey's Figure (immediate and 20-minute delayed recall) (Carlesimo et al., 2002); (3) short-term and working memory: Digit span (forward and backward) and the Corsi Block-Tapping task (forward and backward) (Monaco et al., 2013); (4) executive functions: Phonological Word Fluency (Carlesimo et al., 1996) and Modified Card Sorting Test (Nocentini et al., 2002); (5) language: naming objects subtest of the BADA ("Batteria per l'Analisi dei Deficit Afasici," Italian for "Battery for the analysis of aphasic deficits") (Miceli et al., 1991); (6) Reasoning: Raven's Coloured Progressive Matrices (Carlesimo et al., 1996); (7) constructional praxis: copy of simple drawings with and without landmarks (Carlesimo et al., 1996) and

Table 1
Principal demographic and clinical characteristics of the participants

Mean (SD)	AD	a-MCI	HS	Statistics	*p*-value
	N = 84	N = 48	N = 37		
Age [y]	73.1 (6.2)	71.8 (7.4)	70.7 (5.3)	$F_{2,166} = 1.99$	0.139
Gender (M/F)	34/50	24/24	16/21	$Chi_1^2 < 1.13$	<0.78
Education [y]	9.3 (4.3)[c]	9.9 (4.6)[b]	12.6 (3.5)	$F_{2,166} = 8.01$	0.001
MMSE score	20.4 (4.0)[c,a]	26.1 (1.6)[b]	28.3 (1.9)	$F_{2,166} = 105.05$	0.000
MTA score	2.8 (0.8)[c,a]	2.2 (0.9)[b]	0.7 (0.6)	$F_{2,166} = 88.41$	0.000
Medication: N (%)					
Benzodiazepines	7/84 (8%)	6/48 (12.5%)	-	$Chi_1^2 = 0.6$	0.43
Antidepressants	21/84 (25%)	14/48 (29.1%)	-	$Chi_1^2 = 0.2$	0.63
Neuroleptics	6/84 (7%)	-	-	-	-
AChEIs	35/84 (41.6%)	-	-	-	-

Key: a-MCI, amnestic mild cognitive impairment; AChEIs, Acetylcholinesterase inhibitors; AD, Alzheimer's disease; HS, healthy subjects; MMSE, Mini-Mental State Examination; MTA, medial temporal atrophy scale.
Tukey's post hoc comparisons.
[a] AD versus a-MCI, *p*-value <0.05.
[b] aMCI versus HS, *p*-value <0.05.
[c] AD versus HS, *p*-value <0.05.

copy of Complex Rey's Figure (Carlesimo et al., 2002); (8) general cognitive efficiency: Mini-Mental State Examination (Folstein et al., 1975; Measso et al., 1993). For the purposes of the present study, neuropsychological scores were adjusted for age and education, as reported in the corresponding references. Nineteen one-way ANOVAs were used to assess between-group differences in neuropsychological performances. To avoid the type-I error Bonferroni correction was applied (p value threshold $\alpha = 0.05/19 = 0.003$).

For the neuropsychiatric assessment, AD and a-MCI patients' caregivers were required to complete the Neuropsychiatric Inventory (NPI-12) (Cummings, 1997). This scale assesses the presence and severity of delusions, hallucinations, agitation/aggression, dysphoria/depression, anxiety, euphoria/elation, apathy, disinhibition, irritability/lability, aberrant motor behavior, sleep, and eating disturbances. Each item's score ranges from 0 to 12 and reflects both ratings of severity and frequency of each behavioral symptom, with 0 corresponding to the absence of behavioral symptom and 12 corresponding to its maximum frequency and severity.

A factor analysis was used to extract in AD and a-MCI patients main factors from NPI-12. Factor analysis describes variability among observed correlated variables in terms of a potentially lower number of unobserved variables called factors. In the present case, we hypothesized that the factors represented the common variance in the 12 subscales of NPI-12. Each NPI-12's score (frequency by severity) was entered as variables of interest in factor analyses. Factor analyses were performed using the Maximum Likelihood estimation method (with eigenvalues >1 for the factors' extraction and VARIMAX method for factors' rotation). Factors extracted from NPI-12 were then used in the MRI data analyses.

A trained psychologist screened HS to exclude any psychopathological symptom on the basis of dedicated clinical interviews.

Statistics to assess differences in symptoms' occurrence across patients' subgroups was performed using a series of χ^2 tests.

2.3. MRI acquisition

All imaging was obtained, in a single session, using a head only 3.0 T MRI scanner (Siemens Magnetom Allegra, Siemens Medical Solutions, Erlangen, Germany). The MRI acquisition protocol included (1) a dual-echo turbo spin echo (repetition time [TR] = 6190 ms, echo times [TE] = 12/109 ms, echo train length = 5; matrix = 256 × 192; field of view = 230×172.5 mm^2; 48 contiguous 3 mm thick slices); (2) a fast fluid attenuated inversion recovery (TR = 8170 ms, TE = 96 ms, inversion time = 2100 ms; echo train length = 13; with same field of view, matrix, and number of slices as turbo spin echo), (3) 3D Modified Driven Equilibrium Fourier Transform (MDEFT) scan (TR = 1338 ms, TE = 2.4 ms, matrix = 256 × 224, n slices = 176, thickness = 1 mm), (4) a T2*-weighted echo-planar imaging sensitized to blood oxygenation level dependent contrast (TR = 2080 ms, TE = 30 ms, 32 axial slices parallel to anterior commissure-posterior commissure line, matrix = 64 × 64, pixel size = 3 × 3 mm^2, slice thickness = 2.5 mm, flip angle = 70°) for resting-state fMRI (total number of volumes = 220). During this acquisition, subjects were instructed to keep their eyes closed, not to think of anything in particular, and not to fall asleep.

2.3.1. Medial temporal lobe atrophy

The medial temporal lobe atrophy scale (MTA) (Scheltens et al., 1995) was used to assess on volumetric images (MDEFT), the presence and severity of atrophy in each subject. This scale provides a rating score from 0 to 4, with scores ≥1.5 (Pereira et al., 2004) indicating significant atrophy. For each subject, we averaged the scores obtained in the right and left hemispheres to obtain a single measure of medial temporal lobe atrophy. One-way ANOVA was used to control for between-group differences.

2.3.2. Image analysis of resting-state fMRI data

Images were preprocessed for resting-state fMRI using Statistical Parametric Mapping version 8 (SPM8, http://www.fil.ion.ucl.ac.uk/spm/), and in-house MATLAB scripts as previously described (Bozzali et al., 2015). First, every participant's MDEFT was segmented in SPM8 to obtain participant-specific white matter and cerebrospinal fluid (CSF) masks, as well as to estimate the total grey matter volume.

As both VTA and LC are very small, we followed a pipeline similar to that described by Bär et al. (Bär et al., 2016). For each participant, the first 4 volumes of the fMRI series were discarded to allow for T1 equilibration effects. The preprocessing steps included correction for head motion, compensation for slice-dependent time shifts, and normalization to the echo-planar imaging template in Montreal Neurological Insititute (MNI) coordinates provided with SPM8. For each data set, motion correction was checked to ensure that the maximum absolute shift did not exceed 1.5 mm and the maximum absolute rotation did not exceed 1°. Data sets not fulfilling these criteria were removed. In addition, to minimize the risk that our results were affected by differing degree of motion for the 3 participants' groups, we computed the global correlation (GCORR, Saad et al., 2013), the average mean displacement (root mean square [RMS] of the 6 realignment parameters), and the average framewise displacement (FD, Power et al., 2012) and compared them between

AD and HS, and between MCI and HS, respectively, using independent sample T-tests. The signal in every voxel was regressed against the average white matter and CSF signals, as well as against the 6 realignment parameters. Then, all images were filtered by a phase-insensitive band-pass filter (pass band 0.01–0.08 Hz) to reduce the effect of low-frequency drift and high-frequency physiological noise. We refer to these data sets as unsmoothed corrected data. These data were then smoothed via filtering with a 3D Gaussian kernel with 10 mm^3 full width at half maximum.

2.3.3. Seed-based analyses

Standard space seed masks of the left and right VTA and LC were produced using the Harvard Ascending Arousal Network Atlas in MGH152_1 mm Space (https://www.martinos.org/) (Edlow et al., 2012) (Fig. 1).

The mean time course within each seed region was extracted (from the unsmoothed corrected data) for every participant (averaged for left and right sides). This was done to minimize the partial volume contamination from neighboring nuclei. The smoothed data were then regressed voxelwise against these time courses in a first-level SPM8 analysis (Olivito et al., 2017). The resulting beta images were taken to the second level for a random-effect group analysis. At second level, 2 full factorial models (with a 3-level factor modeling the group) were used to assess between-group differences in VTA and LC FC, separately.

Next, we assessed the potential associations between the NPI-12's factors and FC changes in a-MCI and AD patients using multiple regression models. To do that, we selected some a priori spherical (radius = 6 mm) regions of interest (ROIs), centered in the peak coordinates of the clusters that showed differences in connectivity between patients and controls. The mean connectivity in these areas was extracted and correlated with the 5 factors using Pearson's correlation coefficient. In addition, we performed a more exploratory analysis, looking at the whole brain is SPM. Five separate whole-brain analyses were performed for each factor. In all analyses, whole-brain GM volumes and years of formal education were entered as covariates of no interest. Statistical significance was always set at $p < 0.05$ familywise error corrected at cluster level.

3. Results

3.1. Demographic and clinical characteristics

There were no significant differences between groups in age and gender distribution (Table 1). There were significant differences across groups in years of formal education.

3.2. Neuropsychological assessment

As expected, AD patients showed significantly worse performances than a-MCI patients and HS in each administered test. a-MCI patients showed worse performances than HS in tests assessing episodic memory and executive functions. Details of the neuropsychological assessment are summarized in Table 2.

3.3. Neuropsychiatric assessment

Fig. 2 shows, for the NPI-12 subscale, the percentage of patients who reported a score higher than 0.

As expected, patients with AD showed a significantly higher occurrence than patients with a-MCI in the following NPI-12 subscales: delusions (15 of 84 AD patients [17.8%], vs. 1 of 48 a-MCI patients [2.1%], $\chi^2 = 7.13$, df = 1, $p = 0.007$); agitation (34 of 84 AD patients [40.5%], vs. 11 of 48 a-MCI patients [22.9%], $\chi^2 = 4.19$, df = 1, $p = 0.04$); euphoria (10 of 84 AD patients [11.9%], vs. 1 of 48 a-MCI patients [2.1%], $\chi^2 = 3.86$, df = 1, $p = 0.04$); disinhibition (19 of 84 AD patients [21.4%], vs. 4 of 48 a-MCI patients [4.8%], $\chi^2 = 4.33$, df = 1, $p = 0.03$); motor aberrant behavior (19 of 84 AD patients [21.4%],

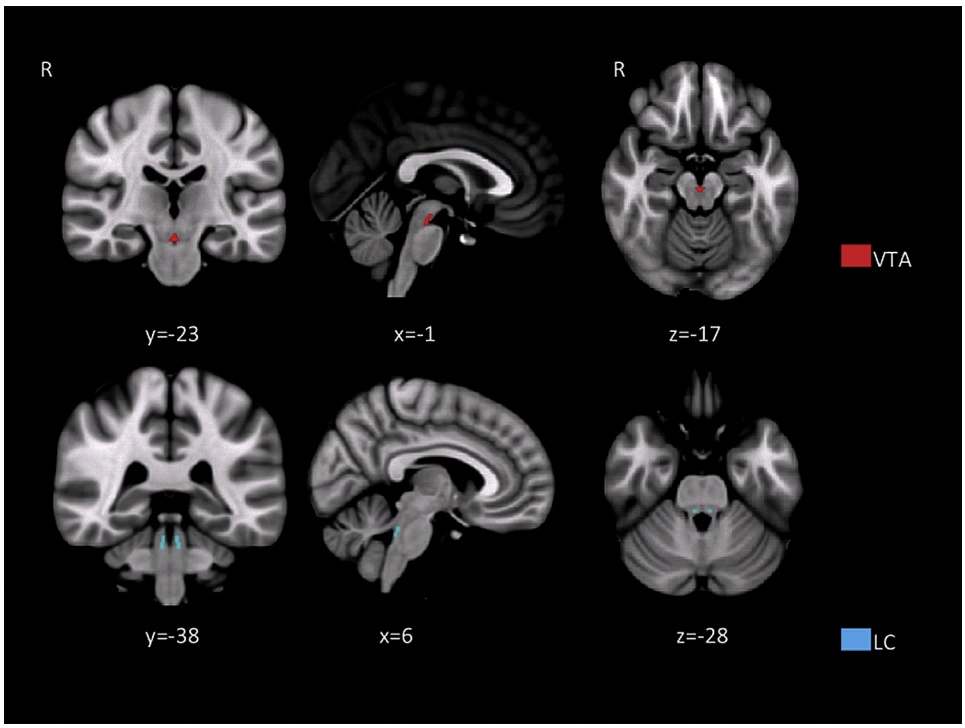

Fig. 1. Seed areas used to assess connectivity in VTA and LC. The figure illustrates the anatomical points used as seed to assess connectivity starting from VTA (in red) and LC (in blue). For the anatomical definition of VTA and LC, the Harvard AAN Atlas has been used (https://www.martinos.org/) (Edlow et al., 2012). For the purpose of the illustration, the VTA and LC are overlaid onto the Ch2bet template using mricron (http://people.cas.sc.edu/rorden/mricron/). Abbreviations: AAN, Ascending Arousal Network; LC, locus coeruleus; VTA, ventral tegmental area. (For interpretation of the references to color in this figure legend, the reader is referred to the Web version of this article.)

Table 2
Performance obtained by participants on neuropsychological testing

Neuropsychological test	AD	a-MCI	HS	F	*p*-value
Verbal episodic memory					
15-Word List:					
Immediate recall (cutoff ≥ 28.5)	24.8 (8.8)[a,b]	30.9 (5.6)[c]	44.6 (8.8)	$F_{2,166} = 77.15$	0.000
Delayed recall (cutoff ≥ 4.6)	2.8 (2.4)[a,b]	4.4 (2.4)[c]	9.4 (2.3)	$F_{2,166} = 94.78$	0.000
Recognition hit rates	8.4 (3.9)[a,b]	10.7 (2.9)[c]	13.3 (1.6)	$F_{2,166} = 25.05$	0.000
Recognition false	6.3 (6.7)[a,b]	5.8 (5.2)[c]	1.7 (1.7)	$F_{2,166} = 7.54$	0.001
Short Story					
Immediate recall (cutoff ≥ 3.1)	1.0 (1.7)[a,b]	3.3 (2.4)[c]	5.3 (1.5)	$F_{2,166} = 55.70$	0.000
Immediate recall (cutoff ≥ 2.8)	1.1 (1.9)[a,b]	3.7 (2.4)[c]	5.5 (1.5)	$F_{2,166} = 50.41$	0.000
Visuospatial episodic memory					
Rey's Complex Figure					
Immediate recall (cutoff ≥ 6.4)	7.2 (5.2)[a,b]	10.9 (6.1)[c]	16.1 (6.6)	$F_{2,166} = 24.66$	0.000
Delayed recall (cutoff ≥ 6.3)	6.0 (5.3)[a,b]	9.9 (6.8)[c]	16.1 (5.6)	$F_{2,166} = 31.41$	0.000
Verbal short-term memory					
Digit Span forward (cutoff ≥ 3.7)	4.8 (1.1)[a]	5.2 (0.9)	5.7 (1.1)	$F_{2,166} = 10.19$	0.001
Digit Span backward	2.8 (1.6)[a,b]	3.6 (1.3)	4.3 (0.7)	$F_{2,166} = 15.53$	0.000
Visuospatial short-term memory					
Corsi Span forward (cutoff ≥ 3.5)	3.8 (1.5)[a,b]	4.5 (0.6)	5.1 (0.8)	$F_{2,166} = 16.03$	0.000
Corsi Span backward	2.8 (1.9)[a,b]	3.7 (1.2)	4.6 (0.9)	$F_{2,166} = 13.61$	0.000
Executive functions					
Phonological verbal fluency (cutoff ≥ 17.3)	23.0 (10.5)[a,b]	29.6 (6.7)[c]	36.3 (10.2)	$F_{2,166} = 25.56$	0.000
Modified Card Sorting Test Criteria achieved (cutoff ≥ 17.3)	2.3 (1.7)[a,b]	3.8 (2.0)[c]	5.7 (0.6)	$F_{2,166} = 43.22$	0.000
Reasoning					
Raven's Progressive Matrices (cutoff ≥ 18.9)	22.6 (8.0)[a,b]	27.0 (4.8)[c]	31.6 (3.7)	$F_{2,166} = 25.26$	0.000
Language					
Naming of objects (cutoff ≥ 22)	24.4 (7.9)[a,b]	28.2 (1.9)	28.5 (2.1)	$F_{2,166} = 8.94$	0.001
Constructional praxis					
Copy of drawings (cutoff ≥ 7.1)	7.6 (3.5)[a,b]	9.5 (1.8)	10.8 (1.1)	$F_{2,166} = 18.15$	0.000
Copy of drawings with landmarks (cutoff ≥ 61.8)	56.8 (19.1)[a,b]	66.5 (3.8)	69.3 (0.8)	$F_{2,166} = 11.55$	0.000
Rey's Complex Figure Copy (cutoff ≥23.7)	22.9 (11.2)[a,b]	29.4 (7.1)	32.3 (3.6)	$F_{2,166} = 14.22$	0.000

Key: a-MCI, amnestic mild cognitive impairment; AD, Alzheimer's disease; HS, healthy subjects.
Tukey's post hoc comparisons.
[a] AD versus HS *p*-value <0.05.
[b] AD versus a-MCI *p*-value <0.05.
[c] a-MCI versus HS *p*-value <0.05.

vs. 1 of 48 a-MCI patients [2.1%], $\chi^2 = 10.0$, df = 1, $p = 0.001$). When adjusting for multiple comparisons using Bonferroni correction (threshold for significance $p = 0.05/12 = 0.004$), only motor aberrant behavior remains significantly different. Interestingly, the 2 groups of patients showed no statistical differences in the high occurrence of the following NPI-12 subscales: depression (43 of 84 AD patients [51.1%], vs. 21 of 48 a-MCI patients [43.7%], $\chi^2 = 0.68$, df = 1, $p = 0.41$); apathy (49 of 84 AD patients [58.3%], vs. 21 of 48 a-MCI patients [43.7%], $\chi^2 = 2.61$, df = 1, $p = 0.11$); anxiety (39 of 84 AD patients [46.4%], vs. 21 of 48 a-MCI patients [43.7%], $\chi^2 = 0.09$, df = 1, $p = 0.77$); irritability (37 of 84 AD patients [44.0%], vs. 18 of 48 a-MCI patients [37.5%], $\chi^2 = 0.54$, df = 1, $p = 0.46$); sleep disorders (23 of 84 AD patients [27.3%], vs. 12 of 48 a-MCI patients [25.0%], $\chi^2 = 0.09$, df = 1, $p = 0.76$); and eating disorders: (23 of 84 AD patients [27.3%], vs. 8 of 48 a-MCI patients [16.7%], $\chi^2 = 1.95$, df = 1, $p = 0.16$). Finally, both patient groups showed low occurrence in hallucinations (4 of 84 AD patients [4.8%], vs. 1 of 48 a-MCI patients [2.1%], $\chi^2 = 0.6$, df = 1, $p = 0.44$).

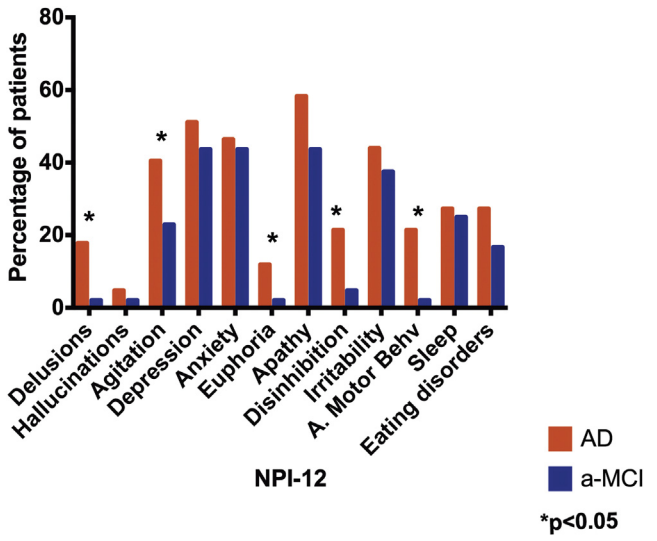

Fig. 2. Neuropsychiatric symptoms in patients with a-MCI and AD. The figure shows the prevalence of behavioral symptoms in a-MCI (in blue) and AD (in red) patients, as assessed by NPI-12. *AD versus a-MCI $p < 0.05$. Abbreviations: a-MCI, amnestic mild cognitive impairment; AD, Alzheimer's disease; NPI-12, Neuropsychiatric inventory-12; A. Motor Behv, aberrant motor behavior. (For interpretation of the references to color in this figure legend, the reader is referred to the Web version of this article.)

Overall, apathy, depression, and anxiety were the most frequent behavioral symptoms observed in our patient cohort, with no significant differences between AD and a-MCI.

From the initial 12 NPI subscales entered in the factor analysis (see Table 3), 5 factors were extracted (54.9% of variance). The NPI-12 subscales reporting a saturation threshold ≥0.35 (Overall and Klett, 1972) were included in a factor as follows: agitation, irritability, and disinhibition in factor 1; hallucination and delusions in factor 2; depression and apathy in factor 3; euphoria and aberrant motor behavior in factor 4; eating and sleep disorders in factor 5.

Based on this classification, 44 patients presented with the symptoms grouped in factor 1 (31 AD and 13 a-MCI; $\chi^2 = 1.33$, df = 1, $p = 0.249$), 22 patients with those in factor 2 (15 AD and 7 a-MCI; $\chi^2 = 0.24$, df = 1, $p = 0.627$), 48 patients with those in factor 3 (31 AD and 17 a-MCI; $\chi^2 = 0.03$, df = 1, $p = 0.864$), 18 patients with those in factor 4 (17 AD and 1 a-MCI; $\chi^2 = 8.55$, df = 1, $p = 0.003$), and 34 patients with those in factor 5 (24 AD and 10 a-MCI; $\chi^2 = 0.96$, df = 1, $p = 0.328$).

Table 3
Results of factor analysis in patients' group

Total variance explained									
Factor	Initial eigenvalues			Extraction sum of squares loadings[a]			Rotate extraction sum of squares loadings[b]		
	Total	% Of variance	% Cumulative	Total	% Of variance	% Cumulative	Total	% Of variance	% Cumulative
1	**3.36**	28.02	28.02	2.22	18.48	18.48	1.67	13.91	13.91
2	**1.60**	13.27	41.30	0.80	6.70	25.17	1.43	11.95	25.85
3	**1.24**	10.30	51.59	1.73	14.42	39.60	1.35	11.27	36.13
4	**1.19**	9.89	61.48	1.18	9.84	49.43	1.19	9.96	47.09
5	**1.02**	8.50	69.98	0.67	5.56	54.99	0.95	7.90	54.99
6	0.88	7.36	77.34						
7	0.69	5.78	83.12						
8	0.55	4.63	87.74						
9	0.49	4.10	91.84						
10	0.38	3.13	94.97						
11	0.37	3.07	98.04						
12	0.23	1.95	100						

Communalities and rotated factor matrix							
	Communalities[a]		Rotated Factor Matrix[b]				
	Initial	Extraction	Factor 1	Factor 2	Factor 3	Factor 4	Factor 5
Delusions	0.29	0.25	0.17	**0.37**	0.25	0.13	0.03
Hallucination	0.48	0.99	−0.01	**0.97**	0.10	0.20	0.09
Agitation	0.43	0.51	**0.67**	0.02	0.19	0.16	−0.03
Depression	0.35	0.84	0.03	0.07	**0.91**	0.04	−0.04
Anxiety	0.17	0.10	0.13	0.06	0.24	−0.04	0.14
Euphoria	0.25	0.18	−0.03	0.18	−0.01	**0.35**	0.14
Apathy	0.36	0.39	0.27	0.09	**0.52**	0.05	0.17
Disinhibition	0.56	0.60	**0.54**	**0.47**	−0.05	0.19	0.24
Irritability	0.53	0.72	**0.80**	0.05	0.23	−0.05	0.14
Ab. Mot Beh.	0.34	0.99	0.23	0.12	0.05	**0.96**	0.07
Sleep	0.21	0.39	−0.03	−0.01	0.11	0.13	**0.60**
Eating disorder	0.41	0.62	0.32	0.26	0.07	0.09	**0.65**

Key: Ab. Mot Beh., aberrant motor behavior.
[a] Extraction method: Maximum likelihood.
[b] Rotation method: Varimax with Kaiser Normalization; the variables in bold included in each factor according to the saturation threshold ≥ 0.35 (Overall and Klett, 1972).

3.4. Medial temporal lobe atrophy

None of the HS showed evidence of clinically relevant hippocampal atrophy (MTA ≤1). All patients (a-MCI and AD) reported MTA scores significantly higher than those reported HS (Table 1).

3.5. Functional brain connectivity

3.5.1. Changes in FC within the brainstem monoaminergic nuclei across AD stages

Four participants with AD, 1 with a-MCI, and 1 HS were removed from the analysis because of excessive movement. After removing them, there were no significant differences between groups in any of the following: GCORR (AD vs. HS, $p = 0.75$; MCI vs. HS, $p = 0.17$); mean motion parameters RMS (AD vs. HS, $p = 0.24$; MCI vs. HS, $p = 0.47$); mean FD (AD vs. HS, $p = 0.51$; MCI vs. HS, $p = 0.47$, and 0.51).

In HS, the VTA was functionally connected to the main nodes of the DMN (see Fig. 3A), while LC was connected to some of the nodes of the salience network (the insular cortices and with basal ganglia) as well as with the orbitofrontal and the parahippocampal cortices (Fig. 3B). Similar patterns were observed also in a-MCI and AD, although qualitatively the connectivity appears reduced.

Quantitatively, compared to HS, patients with a-MCI showed lower FC in VTA and in the right parietal lobule (BA7). AD patients showed lower FC than HS between VTA and the posterior cingulate cortex (PCC), precuneus, and parietal lobule bilaterally (BA7). No changes were found in the opposite direction. These results are summarized in Fig. 4. Conversely, when looking at LC connectivity, there were no between-group changes that reached statistical significance. As discussed below (page 9), this is likely due to the low resolution power of our MRI data to LC whose size is relatively small.

3.5.2. Associations between monoaminergic brainstem nuclei connectivity and prevalence of behavioral symptoms

Based on the results of the group comparison, ROI-based associations were investigated in 3 ROIs: the PCC (MNI coordinates [0 −32 34]), the right angular gyrus (MNI coordinates [38 −68 48]), and the left angular gyrus (MNI coordinates [−36 −74 44]). No significant association was found.

For the whole-brain analysis, significant associations were found between VTA connectivity and behavioral symptoms expressed by factor 1 (i.e., agitation, irritability, and disinhibition) and factor 5 (i.e., sleep and eating disorders). Factor 1 was positively correlated with connectivity between VTA and the right hippocampus, and the cerebellum bilaterally. Factor 5 showed a positive correlation with connectivity between VTA and the left putamen and inferior frontal gyrus (see Fig. 5, green). The same factor was also negatively correlated with FC between VTA and the left caudate (see Fig. 5, magenta).

4. Discussion

Over the last 10 years, it has become increasingly clear that specific brainstem regions play a modulatory role in various cognitive and behavioral aspects that accompany aging (Bartus et al., 1982). Among them, VTA and LC are of particular interest, as they are believed to cooperate in a number of physiological functions from cognition to social behavior (Park et al., 2012). The main goal of this study was to assess whether changes in VTA and LC connectivity—used as a proxy of neuronal loss—are present in AD and may account for higher level dysfunctions, as strongly suggested by animal model evidence (Nobili et al., 2017). VTA degeneration was indeed suggested to precede amyloid plaque

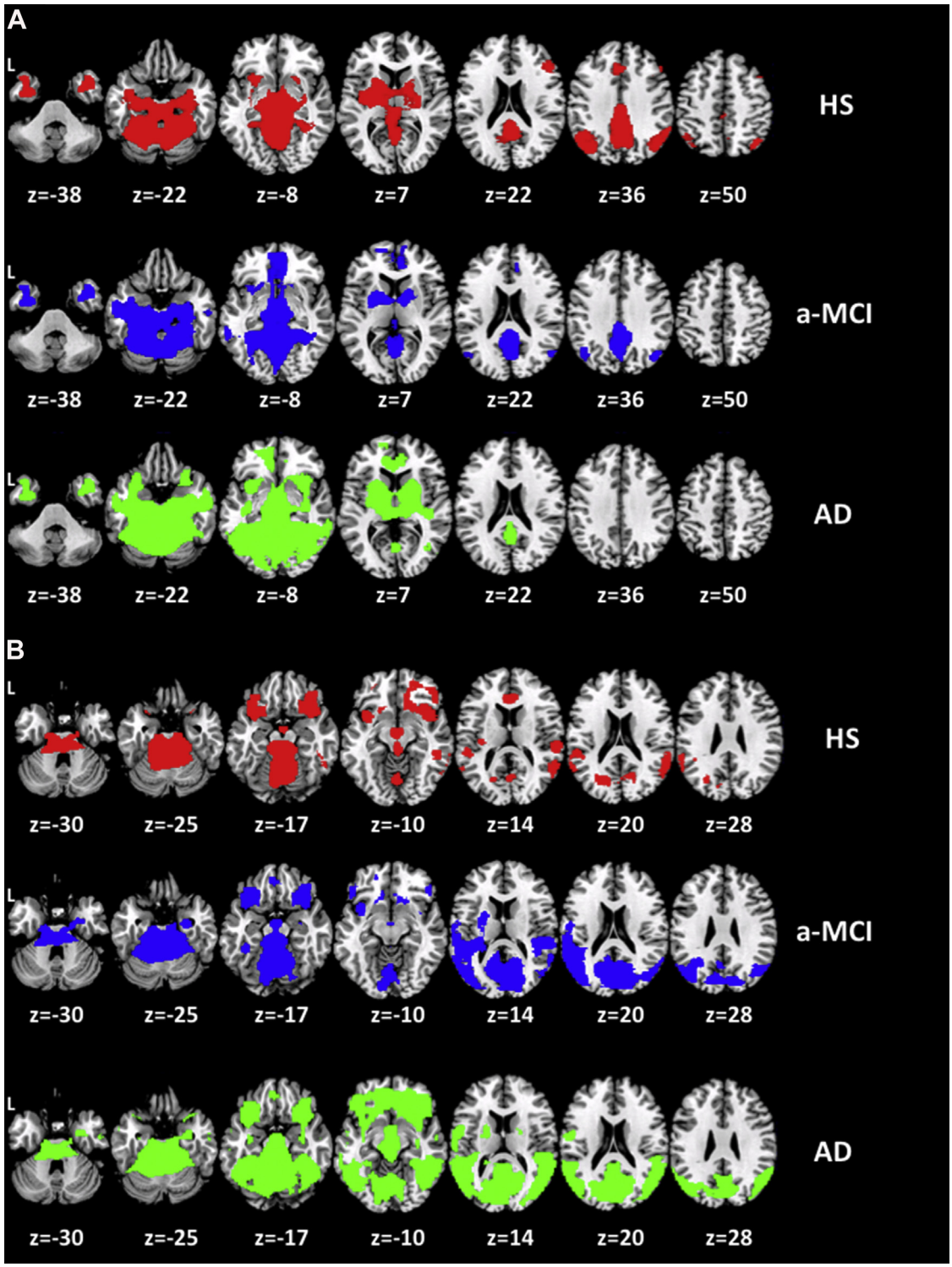

Fig. 3. Patterns of functional connectivity between VTA and LC and the rest of the brain across groups. (A) VTA connectivity. VTA was connected mainly with the nodes of default mode network, with the mediotemporal regions and with basal ganglia (in panel A). This pattern was progressively less significant moving from HS to AD. (B) LC connectivity. LC was connected mainly with the orbito-frontal, the parahippocampal, the insular cortices, and with basal ganglia. The results are overlaid onto the Ch2bet template using mricron (http://people.cas.sc.edu/rorden/mricron/). Abbreviations: a-MCI, amnestic mild cognitive impairment; AD, Alzheimer's disease; FC, functional connectivity; HS, healthy subjects; L, left.

formation, while a very early involvement of LC (Braak and Del Tredici, 2011a; Braak and Del Tredici, 2011b; Theofilas et al., 2017) was demonstrated in AD brains as associated to accumulation of NFT (Andrés-Benito et al., 2017). For this reason, we included in our study patients at early (a-MCI) and intermediate stages of AD. The clinical, radiological (MTA) and neuropsychological characteristics of our sample suggest a diagnosis of Alzheimer's clinical syndrome (Albert et al., 2011; Jack et al., 2018; McKhann et al., 2011). In line with our hypothesis and with previous animal work (Nobili et al., 2017), we found evidence of VTA disconnection with the right

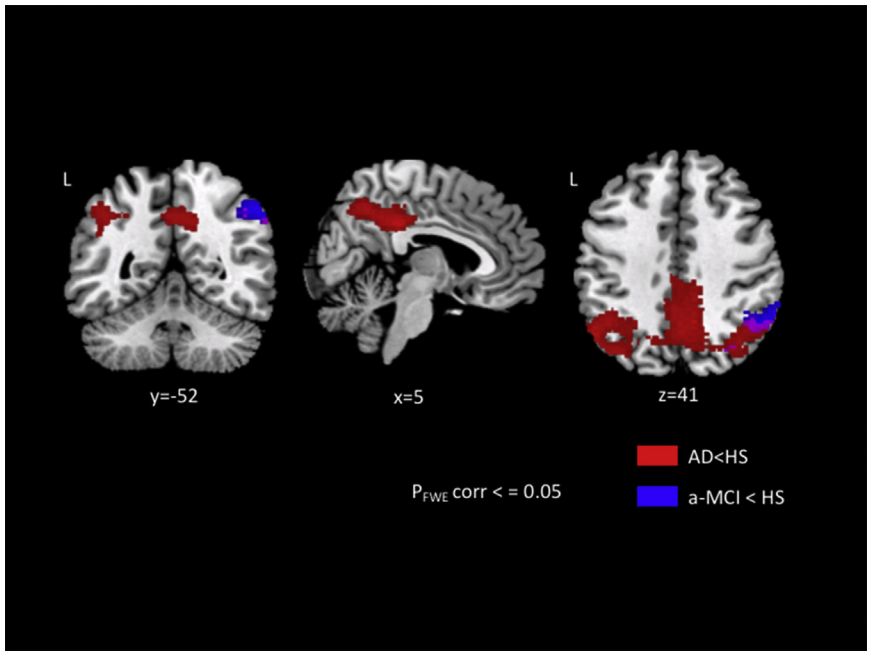

Fig. 4. Reductions in VTA connectivity between patients and healthy controls. Patients with a-MCI compared to HS (in blue) showed reduced FC and the right parietal lobule. AD patients compared to HS (in red) showed lower functional connectivity and PCC, and precuneus and parietal lobules bilaterally. The overlapping areas are shown in purple. The results are FWE-corrected at cluster level ($p < 0.05$) and overlaid onto the Ch2bet template using mricron (http://people.cas.sc.edu/rorden/mricron/). Abbreviations: a-MCI, amnestic mild cognitive impairment; AD, Alzheimer's disease; FC, functional connectivity; FWE, familywise error; HS, healthy subjects; PCC, posterior cingulate cortex; L, left. (For interpretation of the references to color in this figure legend, the reader is referred to the Web version of this article.)

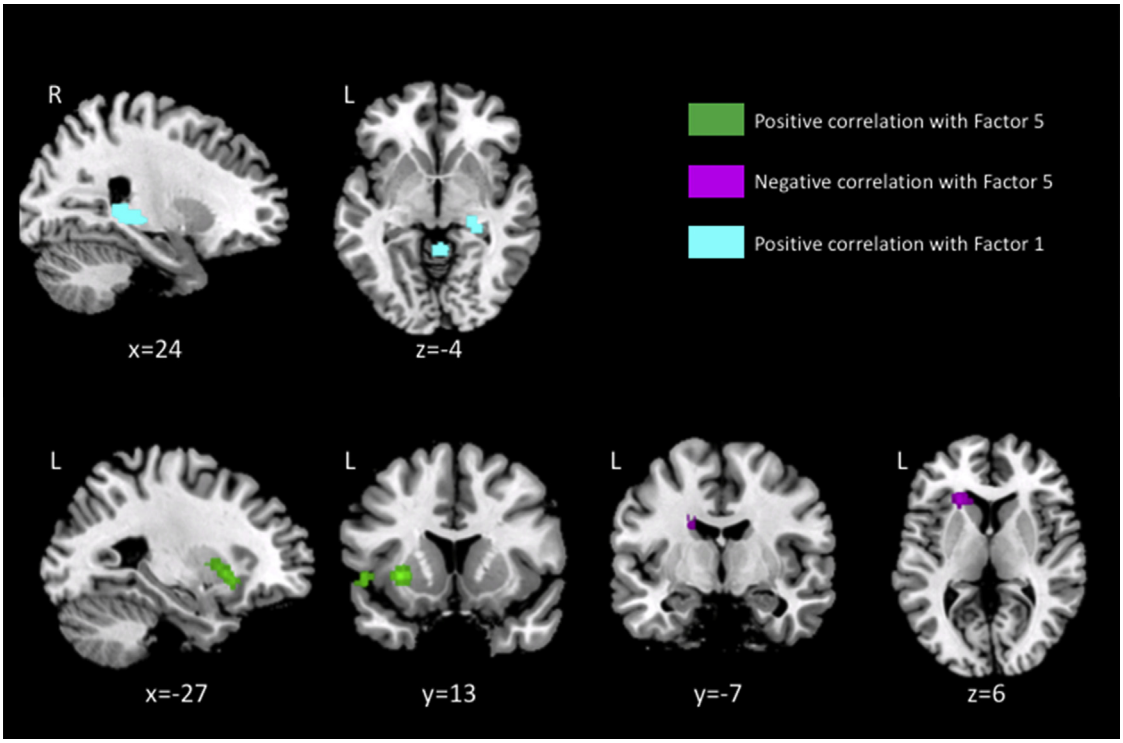

Fig. 5. Correlations between neuropsychiatric factors and VTA connectivity. Of the 5 factors explaining most of the variance in NPI-12 (see text), we found significant associations of VTA connectivity with factor 1 (agitation, irritability, and disinhibition) and with factor 5 (eating and sleep disorders). Direct associations with factor 1 were found in the right hippocampus and the cerebellum bilaterally (top left, in cyan). Both positive (in green) and negative (in magenta) associations were found with factor 5 (bottom), in left putamen/inferior frontal gyrus and the left caudate, respectively. The results are FWE-corrected at cluster level ($p < 0.05$) and overlaid onto the Ch2bet template using mricron (http://people.cas.sc.edu/rorden/mricron/). Abbreviations: FWE, familywise error; L, left. (For interpretation of the references to color in this figure legend, the reader is referred to the Web version of this article.)

parietal lobe (BA7) in a-MCI. These results are consistent with previous observations that degeneration of dopaminergic neurons in VTA is already present in the preplaque mouse model of AD stage (Nobili et al., 2017). In the animal model, VTA degeneration was found to contribute to the memory deficits and dysfunction of reward processing (Nobili et al., 2017), which are regarded as motivated behaviors. In AD, the pattern of VTA disconnection extended to additional parietal areas, with a substantial involvement of the cingulate cortex and precuneus. These findings support the hypothesis of a progressive degeneration on VTA neurons with AD progression. Interestingly, this pattern largely overlaps with the major nodes of the so-called DMN (Gili et al., 2011), including the PCC and precuneus, and the right parietal node. AD patients were characterized by a more extensive disconnection in these areas than patients with a-MCI. It was previously argued that disconnection in the PCC is a critical transitional step for the conversion from a-MCI to AD (Bozzali et al., 2012; Gili et al., 2011). In addition, VTA and the substantia nigra pars compacta were demonstrated being functionally connected to regions of the DMN in healthy controls (Bär et al., 2016). Our current findings suggest that the often reported disconnection within the DMN (Seeley et al., 2009) might not be caused only by loss of neurons from the medial temporal lobes, but also associated with VTA dysfunction. In contrast to our working hypothesis and previous literature (Braak and Del Tredici, 2011a; Braak and Del Tredici, 2011b; Theofilas et al., 2017; Andrés-Benito et al., 2017; Jacobs et al., 2015), we were unable to identify any significant changes in FC between LC and the rest of the brain in both patient groups (at the statistical thresholds chosen for this study). Considering the small size of LC, we argue that this nucleus is below the resolution power of our MRI data, and therefore, we are unable to draw conclusions about LC connectivity in our patient cohort. Admittedly, Jacobs et al. (2015), using resting-state fMRI, have previously reported reduced LC connectivity with the parahippocampal gyrus in patients with a-MCI that correlated with memory performance (Jacobs et al., 2015). There are some technical differences that might at least partially account for the inconsistency of our current results. First, Jacobs and coauthors warped the seed masks into each participant's native space, while we extracted the time series from warped data and then used smoothed data (4 mm full width at half maximum). Second, they used a different method to correct for multiple comparisons. We also observed some connectivity changes in the LC of AD patients when using less stringent statistical thresholds (data not shown).

From a clinical point of view, VTA degeneration has been recently associated to memory dysfunction in AD and a-MCI patients (De Marco & Venneri, 2018). The dopaminergic system is known to be remarkably implicated in behavioral and psychological aspects; thus, the loss of dopaminergic neurons could be particularly relevant for the manifestation of psychiatric symptoms in AD. These symptoms are frequently observed in AD and are known to become increasingly worse along with disease progression (Alves et al., 2017; Masters et al., 2015). Behavioral symptoms have been previously reported also in a-MCI patients, although they have not been univocally associated with neurodegeneration (Gonsalvez et al., 2017; Makovac et al., 2016; Serra et al., 2010). To establish whether VTA degeneration and disconnection could account for behavioral symptoms, we investigated the association between VTA FC and NPI-12 factors. We could not find clear evidence that the loss of connectivity between VTA and the nodes of the DMN impacts on behavioral symptoms. However, in a more exploratory, whole-brain analysis, we found significant associations with factor 5 (including sleep and eating disorders) and with factor 1 (including agitation, irritability and disinhibition). Interestingly, factor 5 showed both increased VTA connectivity mainly in the putamen and reduced connectivity in the caudate. The basal ganglia play a well-known role in regulating sleep and wakefulness (Rolinski et al., 2016), and sleeping disorders are frequently associated with other neurological diseases, such as Parkinson's disease, that affect the basal ganglia. Moreover, reduced activity in the caudate has been found also in the subject suffering from insomnia (Stoffers et al., 2014). In addition, we found also increased connectivity related to factor 1 in the hippocampus and in the cerebellum, 2 brain areas innervated by VTA dopaminergic neurons (Ikai et al., 1992).

The association with the cerebellum is particularly intriguing considered its contribution to the cognitive and neuropsychiatric deficits in AD (Jacobs et al., 2018; Vermeiren et al., 2014) and the role of dopamine in the cerebellum functions beyond the coordination of voluntary motor activity and motor learning. We previously found an association between hippocampal atrophy and positive behavioral symptoms in patients with AD (Serra et al., 2010). Unexpectedly, the direction of this correlation suggests that increased connectivity between these areas and VTA are associated with worsening in behavioral symptoms. As we did not find any evidence of increased connectivity between the areas of the DMN and VTA, an intriguing interpretation (although very speculative at this stage) is that disengagement of the VTA from the DMN might lead to an increased connectivity between the same area and the salience network.

This study also suffers from some limitations. First of all, VTA and LC are very small nuclei, and they are difficult to identify on MRI. It is therefore possible that some of our results are affected by partial volume with neighboring structures of the brainstem. Nevertheless, we have tried to minimize these effects by extracting the time series from unsmoothed data. Another potential confound comes from respiration and pulsatility artifacts, to which these areas are particularly susceptible. Ideally, these can be accounted for when acquiring respiration data concomitant with fMRI. Unfortunately, we did not have these data. We could have also adopted more sophisticated postprocessing approaches, such as regressing out GCORR (Saad et al., 2013) or complementing whole-brain coregistration with a further, brainstem-weighted registration (Napadow et al., 2006). Nevertheless, the comparisons we computed for 3 parameters reflecting global motion (GCORR, RMS, and FD) suggest that it was comparable among groups. Third, we defined the nuclei using an atlas in standard space (due to the aforementioned difficulties in identifying each nucleus on subject-specific MRI). A more accurate location could have been achieved by registering the standard ROI to each participant's scan (Jacobs et al., 2015). In addition, if the nuclei under observation are characterized by macroscopic atrophy, it is possible that this might influence the results of our connectivity analysis. However, for the motivations explained previously, it is not possible to measure the volume of each nucleus independently, and thus adjust for this potential confound. Finally, we did not have access to information of amyloid in our cohort, either from CSF analysis or photon emission tomography imaging. This information would increase the diagnostic confidence, particularly in view of the most recent criteria, which require amyloid and tau biomarkers for the diagnosis of AD (Jack et al., 2018). Unfortunately, these biomarkers were not available in our cohort of patients and this is a limitation of the study. It is therefore possible that some of the participants might have other forms of dementia, such as fronto-temporal lobar degeneration. Nevertheless, this is highly unlikely because the whole cohort showed clinical (episodic memory disorder at onset), radiological (hippocampal atrophy) and neuropsychological (memory disorders confirmed by formal tests) features suggesting the presence of an Alzheimer's clinical syndrome at different clinical stages (Albert et al., 2011; Jack et al., 2018; McKhann et al., 2011).

In addition, despite the performance of patients with AD at language tests (naming of objects) being significantly worse than

that of controls and a-MCI participants, on average, it was still within the range of normality (mean = 24, cutoff = 22), thus minimizing the likelihood that they had frontotemporal degeneration. Because of the specific focus of this study, it would have been useful also to measure dopamine levels to support the MRI findings.

In summary, the present study has identified a progressive functional disconnection between VTA and several brain regions, measurable since the a-MCI stage. These FC changes are likely to reflect a progressive dopaminergic dysregulation, and it might account for several behavioral symptoms, including circadian disorders and agitation, irritability, and disinhibition observed in both a-MCI and AD patients. Although the role of dopaminergic system in early AD patients is not fully explored, this clinical investigation providing compelling evidence of altered connectivity between VTA and some key brain regions involved in AD pathology.

Disclosure statement

The authors have no conflicts of interest to disclose.

Acknowledgements

The Neuroimaging Laboratory is in part supported by the Italian Ministry of Health. MDA was supported by the Italian Ministry of Health (Progetto Giovani Ricercatori Project Code GR-2011-02351457) and by a grant from the Alzheimer's Association, United States (Project Code AARG-18-566270s).

References

Albert, M.S., DeKosky, S.T., Dickson, D., Dubois, B., Feldman, H.H., Fox, N.C., Gamst, A., Holtzman, D.M., Jagust, W.J., Petersen, R.C., Snyder, P.J., Carrillo, M.C., Thies, B., Phelps, C.H., 2011. The diagnosis of mild cognitive impairment due to Alzheimer's disease: recommendations from the National Institute on Aging-Alzheimer's Association workgroups on diagnostic guidelines for Alzheimer's disease. Alzheimers Dement. 7, 270–279.

Alves, G.S., Carvalho, A.F., de Amorim de Carvalho, L., Sudo, F.K., Siqueira-Neto, J.I., Oertel-Knochel, V., Jurcoane, A., Knochel, C., Boecker, H., Laks, J., Pantel, J., 2017. Neuroimaging findings related to behavioral disturbances in Alzheimer's disease: a systematic review. Curr. Alzheimer Res. 14, 61–75.

Andrés-Benito, P., Fernández-Dueñas, V., Carmona, M., Escobar, L.A., Torrejón-Escribano, B., Aso, E., Ciruela, F., Ferrer, I., 2017. Locus coeruleus at asymptomatic early and middle Braak stages of neurofibrillary tangle pathology. Neuropathol. Appl. Neurobiol. 43, 373–392.

American Psychiatric Association (APA), 2013. Diagnostic and Statistical Manual of Mental Disorders, DSM-fifth ed. American Psychiatric Association, Arlington, VA.

Ashok, A.H., Marques, T.R., Jauhar, S., Nour, M.M., Goodwin, G.M., Young, A.H., Howes, O.D., 2017. The dopamine hypothesis of bipolar affective disorder: the state of the art and implications for treatment. Mol. Psychiatry 22, 666–679.

Bär, K.J., de la Cruz, F., Schumann, A., Koehler, S., Sauer, H., Critchley, H., Wagner, G., 2016. Functional connectivity and network analysis of midbrain and brainstem nuclei. Neuroimage 134, 53–63.

Bartus, R.T., Dean, R.L., Beer, B., Lippa, A.S., 1982. The cholinergic hypothesis of geriatric memory dysfunction. Science 217, 408–414.

Benussi, A., Di Lorenzo, F., Dell'Era, V., Cosseddu, M., Alberici, A., Caratozzolo, S., Cotelli, M.S., Micheli, A., Rozzini, L., Depari, A., Flammini, A., Ponzo, V., Martorana, A., Caltagirone, C., Padovani, A., Koch, G., Borroni, B., 2017. Transcranial magnetic stimulation distinguishes Alzheimer disease from frontotemporal dementia. Neurology 89, 665–672.

Bianciardi, M., Strong, C., Toschi, N., Edlow, B.L., Fischl, B., Brown, E.N., Rosen, B.R., Wald, L.L., 2018. A probabilistic template of human mesopontine tegmental nuclei from in vivo 7T MRI. Neuroimage 170, 222–230.

Biswal, B., Yetkin, F.Z., Haughton, V.M., Hyde, J.S., 1995. Functional connectivity in the motor cortex of resting human brain using echo-planar MRI. Magn. Reson. Med. 34, 537–541.

Borodovitsyna, O., Flamini, M., Chandler, D., 2017. Noradrenergic modulation of cognition in Health and disease. Neural Plast. 2017, 6031478.

Bozzali, M., Dowling, C., Serra, L., Spanò, B., Torso, M., Marra, C., Castelli, D., Dowell, N.G., Koch, G., Caltagirone, C., Cercignani, M., 2015. The impact of cognitive reserve on brain functional connectivity in Alzheimer's disease. J. Alzheimers Dis. 44, 243–250.

Bozzali, M., Giulietti, G., Basile, B., Serra, L., Spanò, B., Perri, R., Giubilei, F., Marra, C., Caltagirone, C., Cercignani, M., 2012. Damage to the cingulum contributes to Alzheimer's disease pathophysiology by deafferentation mechanism. Hum. Brain Mapp. 33, 1295–1308.

Braak, H., Del Tredici, K., 2011a. Alzheimer's pathogenesis: is there neuron-to-neuron propagation? Acta Neuropathol. 121, 589–595.

Braak, H., Del Tredici, K., 2011b. The pathological process underlying Alzheimer's disease in individuals under thirty. Acta Neuropathol. 121, 171–181.

Büsch, D., Hagemann, N., Bender, N., 2010. The dimensionality of the Edinburgh Handedness Inventory: an analysis with models of the item response theory. Laterality 15, 610–628.

Carlesimo, G.A., Buccione, I., Fadda, L., Graceffa, A., Mauri, M., Lorusso, S., Bevilacqua, G., Caltagirone, C., 2002. Standardizzazione di due test di memoria per uso clinico: Breve Racconto e Figura di Rey. Nuova Rivista di Neurologia 12, 1–13.

Carlesimo, G.A., Caltagirone, C., Gainotti, G., 1996. The Mental Deterioration Battery: normative data, diagnostic reliability and qualitative analyses of cognitive impairment. The Group for the Standardization of the Mental Deterioration Battery. Eur. Neurol. 36, 378–384.

Chong, T.T., Husain, M., 2016. The role of dopamine in the pathophysiology and treatment of apathy. Prog. Brain Res. 229, 389–426.

Cummings, J.L., 1997. The Neuropsychiatric Inventory: assessing psychopathology in dementia patients. Neurology 48, S10–S16.

De Marco, M., Venneri, A., 2018. Volume and connectivity of the ventral tegmental area are linked to neurocognitive signatures of Alzheimer's disease in humans. J. Alzheimers Dis. 63, 167–180.

Eban-Rothschild, A., Rothschild, G., Giardino, W.J., Jones, J.R., de Lecea, L., 2016. VTA dopaminergic neurons regulate ethologically relevant sleep-wake behaviors. Nat. Neurosci. 19, 1356–1366.

Edlow, B.L., Takahashi, E., Wu, O., Benner, T., Dai, G., Bu, L., Grant, P.E., Greer, D.M., Greenberg, S.M., Kinney, H.C., Folkerth, R.D., 2012. Neuroanatomic connectivity of the human ascending arousal system critical to consciousness and its disorders. J. Neuropathol. Exp. Neurol. 71, 531–546.

Folstein, M.F., Folstein, S.E., McHugh, P.R., 1975. 'Mini-mental state'. A practical method for grading the cognitive state of patients for the clinician. J. Psychiatr. Res. 12, 189–198.

Fox, M.D., Snyder, A.Z., Vincent, J.L., Corbetta, M., Van Essen, D.C., Raichle, M.E., 2005. The human brain is intrinsically organized into dynamic, anticorrelated functional networks. Proc. Natl. Acad. Sci. U. S. A. 102, 9673–9678.

Francis, P.T., Palmer, A.M., Sims, N.R., Bowen, D.M., Davison, A.N., Esiri, M.M., Neary, D., Snowden, J.S., Wilcock, G.K., 1985. Neurochemical studies of early-onset Alzheimer's disease. Possible influence on treatment. N. Engl. J. Med. 313, 7–11.

Gili, T., Cercignani, M., Serra, L., Perri, R., Giove, F., Maraviglia, B., Caltagirone, C., Bozzali, M., 2011. Regional brain atrophy and functional disconnection across Alzheimer's disease evolution. J. Neurol. Neurosurg. Psychiatry 82, 58–66.

Gonsalvez, I., Baror, R., Fried, P., Santarnecchi, E., Pascual-Leone, A., 2017. Therapeutic noninvasive brain stimulation in Alzheimer's disease. Curr. Alzheimer Res. 14, 362–376.

Hachinski, V.C., Iliff, L.D., Zilhka, E., Du Boulay, G.H., McAllister, V.L., Marshall, J., Russell, R.W., Symon, L., 1975. Cerebral blood flow in dementia. Arch. Neurol. 3, 632–637.

Heneka, M.T., Ramanathan, M., Jacobs, A.H., Dumitrescu-Ozimek, L., Bilkei-Gorzo, A., Debeir, T., Sastre, M., Galldiks, N., Zimmer, A., Hoehn, M., Heiss, W.D., Klockgether, T., Staufenbiel, M., 2006. Locus ceruleus degeneration promotes Alzheimer pathogenesis in amyloid precursor protein 23 transgenic mice. J. Neurosci. 26, 1343–1354.

Hughes, C.P., Berg, L., Danziger, W.L., Coben, L.A., Martin, R.L., 1982. A new clinical scale for the staging of dementia. Br. J. Psychiatry 140, 566–572.

Ikai, Y., Takada, M., Shinonaga, Y., Mizuno, N., 1992. Dopaminergic and non-dopaminergic neurons in the ventral tegmental area of the rat project, respectively, to the cerebellar cortex and deep cerebellar nuclei. Neuroscience 51, 719–728.

Jack Jr., C.R., Bennett, D.A., Blennow, K., Carrillo, M.C., Dunn, B., Haeberlein, S.B., Holtzman, D.M., Jagust, W., Jessen, F., Karlawish, J., Liu, E., Molinuevo, J.L., Montine, T., Phelps, C., Rankin, K.P., Rowe, C.C., Scheltens, P., Siemers, E., Snyder, H.M., Sperling, R., NIA-AA Research Framework, 2018. Toward a biological definition of Alzheimer's disease. Alzheimers Dement. 14, 535–562.

Jacobs, H.I., Wiese, S., van de Ven, V., Gronenschild, E.H., Verhey, F.R., Matthews, P.M., 2015. Relevance of parahippocampal-locus coeruleus connectivity to memory in early dementia. Neurobiol. Aging 36, 618–626.

Jacobs, H.I.L., Hopkins, D.A., Mayrhofer, H.C., Bruner, E., van Leeuwen, F.W., Raaijmakers, W., Schmahmann, J.D., 2018. The cerebellum in Alzheimer's disease: evaluating its role in cognitive decline. Brain 141, 37–47.

Kessler, R.M., Hutson, P.H., Herman, B.K., Potenza, M.N., 2016. The neurobiological basis of binge-eating disorder. Neurosci. Biobehav. Rev. 63, 223–238.

Kim, J., Jang, S., Choe, H.K., Chung, S., Son, G.H., Kim, K., 2017. Implications of circadian rhythm in dopamine and mood regulation. Mol. Cells 40, 450–456.

Köhler, C.A., Magalhaes, T.F., Oliveira, J.M., Alves, G.S., Knochel, C., Oertel-Knöchel, V., Pantel, J., Carvalho, A.F., 2016. Neuropsychiatric disturbances in mild cognitive impairment (MCI): a systematic review of population-based studies. Curr. Alzheimer Res. 13, 1066–1082.

Krebs, R.M., Heipertz, D., Schuetze, H., Duzel, E., 2011. Novelty increases the mesolimbic functional connectivity of the substantia nigra/ventral tegmental area (SN/VTA) during reward anticipation: evidence from high-resolution fMRI. Neuroimage 58, 647–655.

Makovac, E., Serra, L., Spanò, B., Giulietti, G., Torso, M., Cercignani, M., Caltagirone, C., Bozzali, M., 2016. Different patterns of correlation between grey

and white matter integrity account for behavioral and psychological symptoms in Alzheimer's disease. J. Alzheimers Dis. 50, 591–604.
Masters, M.C., Morris, J.C., Roe, C.M., 2015. Noncognitive" symptoms of early Alzheimer disease: a longitudinal analysis. Neurology 84, 617–622.
McKhann, G.M., Knopman, D.S., Chertkow, H., Hyman, B.T., Jack Jr., C.R., Kawas, C.H., Klunk, W.E., Koroshetz, W.J., Manly, J.J., Mayeux, R., Mohs, R.C., Morris, J.C., Rossor, M.N., Scheltens, P., Carrillo, M.C., Thies, B., Weintraub, S., Phelps, C.H., 2011. The diagnosis of dementia due to Alzheimer's disease: recommendations from the National Institute on Aging-Alzheimer's Association workgroups on diagnostic guidelines for Alzheimer's disease. Alzheimers Dement. 7, 263–269.
Measso, G., Cavarzeran, F., Zappalà, G., Grigoletto, F., 1993. The Mini-mental state Examination: normative study of an Italian random sample. Dev. Neuropsychol. 9, 77–85.
Miceli, G., Laudanna, A., Burani, C., Capasso, R., 1991. Batteria per l'analisi dei deficit afasici. Associazione per lo sviluppo delle ricerche neuropsicologiche. Berdata, Milano.
Monaco, M., Costa, A., Caltagirone, C., Carlesimo, G.A., 2013. Forward and backward span for verbal and visuo-spatial data: standardization and normative data from an Italian adult population. Neurol. Sci. 34, 749–754.
Napadow, V., Dhond, R., Kennedy, D., Hui, K.K., Makris, N., 2006. Automated brainstem co-registration (ABC) for MRI. Neuroimage 32, 1113–1119.
Nobili, A., Latagliata, E.C., Viscomi, M.T., Cavallucci, V., Cutuli, D., Giacovazzo, G., Krashia, P., Rizzo, F.R., Marino, R., Federici, M., De Bartolo, P., Aversa, D., Dell'Acqua, M.C., Cordella, A., Sancandi, M., Keller, F., Petrosini, L., Puglisi-Allegra, S., Mercuri, N.B., Coccurello, R., Berretta, N., D'Amelio, M., 2017. Dopamine neuronal loss contributes to memory and reward dysfunction in a model of Alzheimer's disease. Nat. Commun. 8, 14727.
Nocentini, U., Di Vincenzo, S., Panella, M., Caltagirone, C., 2002. La valutazione delle funzioni esecutive nella pratica neuropsicologica: Dal Modified Card Sorting Test al modified card sorting test - Roma version. Dati di standardizzazione. Nuova Rivista di Neurologia 12, 14–24.
Olivito, G., Clausi, S., Laghi, F., Tedesco, A.M., Baiocco, R., Mastropasqua, C., Molinari, M., Cercignani, M., Bozzali, M., Leggio, M., 2017. Resting-state functional connectivity changes between dentate nucleus and cortical social brain regions in autism spectrum disorders. Cerebellum 16, 283–292.
Overall, J.E., Klett, C.J., 1972. Applied Multivariate Analysis. McGraw-Hill Book Company, New York.
Pamphlett, R., Kum Jew, S., 2015. Different populations of human locus ceruleus neurons contain heavy metals or hyperphosphorylated tau: implications for amyloid-β and tau pathology in Alzheimer's disease. J. Alzheimers Dis. 45, 437–447.
Park, J., Wheeler, R.A., Fontillas, K., Keithley, R.B., Carelli, R.M., Wightman, R.M., 2012. Catecholamines in the bed nucleus of the stria terminalis reciprocally respond to reward and aversion. Biol. Psychiatry 71, 327–334.
Pereira, J.B., Cavallin, L., Spulber, G., Aguilar, C., Mecocci, P., Vellas, B., Tsolaki, M., Kłoszewska, I., Soininen, H., Spenger, C., Aarsland, D., Lovestone, S., Simmons, A., Wahlund, L.O., Westman, E., 2004. Influence of age, disease onset and ApoE4 on visual medial temporal lobe atrophy cut-offs. Intern. Med. 275, 317–330.
Power, J.D., Barnes, K.A., Snyder, A.Z., Schlaggar, B.L., Petersen, S.E., 2012. Spurious but systematic correlations in functional connectivity MRI networks arise from subject motion. NeuroImage 59, 2142–2154.
Robertson, S.D., Plummer, N.W., de Marchena, J., Jensen, P., 2013. Developmental origins of central norepinephrine neuron diversity. Nat. Neurosci. 16, 1016–1023.
Rolinski, M., Griffanti, L., Piccini, P., Roussakis, A.A., Szewczyk-Krolikowski, K., Menke, R.A., Quinnell, T., Zaiwalla, Z., Klein, J.C., Mackay, C.E., Hu, M.T., 2016. Basal ganglia dysfunction in idiopathic REM sleep behaviour disorder parallels that in early Parkinson's disease. Brain 139, 2224–2234.
Saad, Z.S., Reynolds, R.C., Jo, H.J., Gotts, S.J., Chen, G., Martin, A., Cox, R.W., 2013. Correcting brain-wide correlation differences in resting-state FMRI. Brain Connect. 3, 339–352.
Schaeffer, E., Berg, D., 2017. Dopaminergic therapies for non-motor symptoms in Parkinson's disease. CNS Drugs 31, 551–570.
Scheltens, P., Launer, L.J., Barkhof, F., Weinstein, H.C., van Gool, W.A., 1995. Visual assessment of medial temporal lobe atrophy on magnetic resonance imaging: interobserver reliability. J. Neurol. 242, 557–560.
Seeley, W.W., Crawford, R.K., Zhou, J., Miller, B.L., Greicius, M.D., 2009. Neurodegenerative diseases target large-scale human brain networks. Neuron 62, 42–52.
Serra, L., Perri, R., Cercignani, M., Spanò, B., Fadda, L., Marra, C., Carlesimo, G.A., Caltagirone, C., Bozzali, M., 2010. Are the behavioral symptoms of Alzheimer's disease directly associated with neurodegeneration? J. Alzheimers Dis. 21, 627–639.
Stoffers, D., Altena, E., van der Werf, Y.D., Sanz-Arigita, E.J., Voorn, T.A., Astill, R.G., Strijers, R.L., Waterman, D., Van Someren, E.J., 2014. The caudate: a key node in the neuronal network imbalance of insomnia? Brain 137, 610–620.
Storga, D., Vrecko, K., Birkmayer, J.G., Reibnegger, G., 1996. Monoaminergic neurotransmitters, their precursors and metabolites in brains of Alzheimer patients. Neurosci. Lett. 203, 29–32.
Theofilas, P., Dunlop, S., Heinsen, H., Grinberg, L.T., 2015. Turning on the light within: subcortical nuclei of the isodentritic core and their role in Alzheimer's disease pathogenesis. J. Alzheimers Dis. 46, 17–34.
Theofilas, P., Ehrenberg, A.J., Dunlop, S., Di Lorenzo Alho, A.T., Nguy, A., Leite, R.E.P., Rodriguez, R.D., Mejia, M.B., Suemoto, C.K., Ferretti-Rebustini, R.E.L., Polichiso, L., Nascimento, C.F., Seeley, W.W., Nitrini, R., Pasqualucci, C.A., Jacob Filho, W., Rueb, U., Neuhaus, J., Heinsen, H., Grinberg, L.T., 2017. Locus coeruleus volume and cell population changes during Alzheimer's disease progression: a stereological study in human postmortem brains with potential implication for early-stage biomarker discovery. Alzheimers Dement. 13, 236–246.
Vermeiren, Y., Van Dam, D., Aerts, T., Engelborghs, S., De Deyn, P.P., 2014. Brain region-specific monoaminergic correlates of neuropsychiatric symptoms in Alzheimer's disease. J. Alzheimers Dis. 41, 819–833.